Rational Engineering of a Schiff Base-Iridium(III) Complex for Enhanced Photodynamic Therapy

Changlin Li,[a#] Xuan Liu,[a#] Tao Shao,[d#] Guodang Chen,[a] Jingran Xuan,[a] Dong Wang,[e*] Zhenbao Li,[abc*] Zhihui Feng[abc*]

[a.] College of Pharmacy, Anhui University of Chinese Medicine, Hefei 230012, China.

[b.] Anhui Province Key Laboratory of Pharmaceutical Preparation Technology and Application, Hefei 230012, China.

[c.] Anhui Province Key Laboratory of the Application and Transformation of Traditional Chinese Medicine in the Prevention and Treatment of Major Pulmonary Diseases

[d.] College of Pharmaceutical Sciences, Anhui Xinhua University, Hefei 230088, China

[e.] School of Chemistry and Chemical Engineering, Anqing Normal University and Anhui Provincial Key Laboratory of Advanced Catalysis and Energy Materials, Anqing, 246003, P.R. China.

[#] C. L. Li, X. Liu and T. Shao are contributed equally to the work.

[*] Corresponding authors: fzh@ahtcm.edu.cn, lizhenbao@ahtcm.edu.cn, wangdongkbz@163.com.

1. Detection of $^1O_2$ by absorbance method

ABDA was used to monitor $^1O_2$ production. In detail, NCN, Ir-NCN and Ce-6 (10 μM) in aqueous solution were prepared in the UV cuvette. Then, ABDA (7.5 mM) was added into the above solution after irradiated with a white light for different time (0 - 100 s). The change in the absorption intensity of the indicator ABDA at 378 nm was monitored.

The $^1O_2$ quantum yields (Φ) of NCN, Ir-NCN and Ce-6 were detected according to the procedure reported previously. [1] The measurements were performed with ABDA as the $^1O_2$ indicator and Rose Bengal (Φ_{RB} = 0.75 in water) as the reference. The quantum yield for each photosensitizer (Φ_{PS}) was calculated according to the following equation:

$$\Phi_{PS} = \Phi_{RB}\frac{K_{PS} \cdot A_{RB}}{K_{RB} \cdot A_{PS}}$$

Here, where K_{PS} and K_{RB} are the decomposition rate constants of ABDA by the PSs and RB, respectively. A_{PS} and A_{RB} represent the light absorbed by the PSs and RB, respectively, which are determined by the integration of the areas under the absorption bands in the wavelength range of 400-700 nm.

2. Cell culture.

Human hepatoma cells (HepG2) were obtained from the Shanghai Institute of Biochemistry and Cell Biology, Chinese Academy of Sciences. The cells were maintained in Dulbecco's modified Eagle's medium (DMEM; Gibco) containing 4.5 g/L glucose and supplemented with 10% fetal bovine serum (FBS; Umedium, Hefei, China), 100 U/mL penicillin, 100 μg/mL streptomycin, and 4 mM L-glutamine. Cultures were incubated at 37 °C in a humidified atmosphere of 5% CO_2 and 95% air.

3. Dark toxicity and phototoxicity assay.

HepG2 cells were seeded in a 96-well plate at an initial density of 5×10^4 cells per well and cultured for 24 h. The cells were then treated with various concentrations of Ir-NCN. After 12 h of incubation, the cells were directly exposed to an 400-700 nm laser (10 mW cm^{-2}) for 5 min. Cells not subjected to laser irradiation were used for

dark toxicity assays. Following further culture for 12 h, CCK-8 reagent was added to each well. Finally, cell viability was measured using a microplate reader at a detection wavelength of 450 nm. The results are expressed as the survival rate of treated cells relative to untreated control cells. The relative cell viability was calculated as follows:

$$Cell\ viability\ (\%) = \frac{ODsample - ODbackground}{ODcontrol - ODbackground} \times 100\%$$

4. Confocal imaging of cells.

HepG2 cells in the logarithmic growth phase were seeded into confocal dishes at a density of 5×10^4 cells/well and cultured in DMEM complete medium supplemented with 10% FBS for 24 h at 37 ℃ under 5% CO_2 to allow cell adherence. After incubation, the old medium was aspirated, and the cells were gently washed once with PBS. The experimental group was treated with Ir-NCN (10 μM), while the control group received an equal volume of PBS. All cells were then returned to the incubator and protected from light for 10 min. Following incubation, the drug-containing medium was carefully removed. A SOSG fluorescent probe working solution (2 μM), diluted in serum-free medium, was added to cover the cells completely, followed by further incubation in the dark at 37℃ for 15 min. The dishes were exposed to specific LED light irradiation (λ_{ex} = 400-700 nm, 10 mW/cm², 10 min) for photostimulation. Control samples were kept strictly protected from light. ROS generation was dynamically monitored immediately using confocal microscopy. Under light-protected conditions, a dual-staining working solution was prepared by diluting Calcein-AM (2 μM) and PI (4 μM) in PBS or serum-free medium. After the drug incubation period, the drug-containing medium was carefully aspirated, and the cells were gently washed once with PBS. The freshly prepared Calcein-AM/PI working solution was then added to completely cover the cells, followed by incubation at 37 °C in the dark for 15 min. After incubation, the staining solution was removed and replaced with PBS. The culture dishes were exposed to specific light irradiation for phototreatment. Control samples were strictly protected from light throughout. Subsequently, observation and image acquisition were performed using a

confocal microscope. The staining procedure using the FITC/PI dual dye is similar to that of the Calcein-AM/PI method and therefore will not be repeated here.

5. Synthesis and characterization of NCN and Ir-NCN

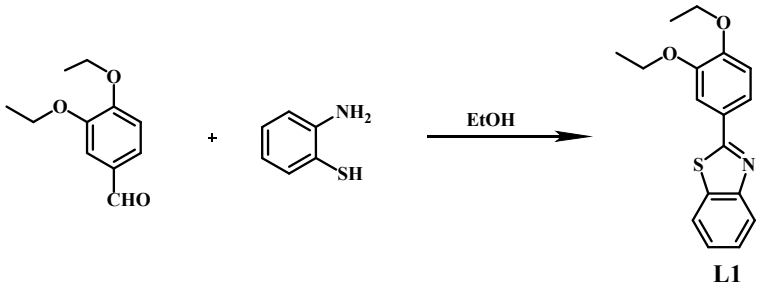

Figure. S1 The synthesis process of ligand **L1**.

Synthesis of L1: The ligand **L1** was synthesized according to the literature[2].

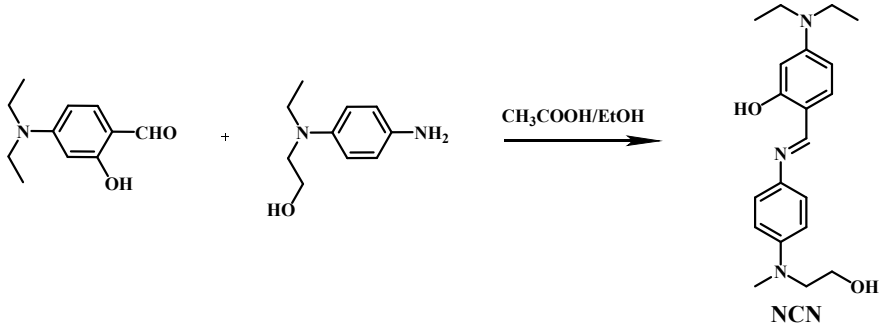

Figure. S2 The synthesis process of ligand **NCN**.

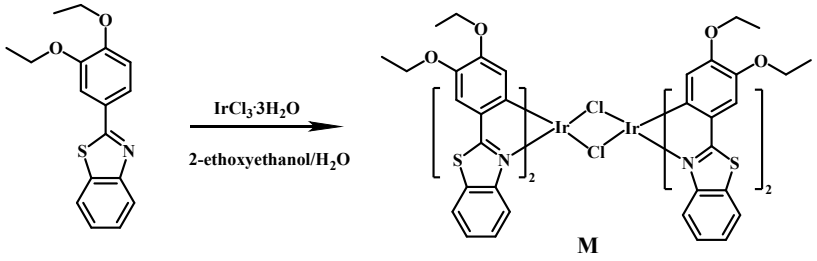

Figure. S3 The synthesis process of the tintermediate **M**.

Synthesis of M: The intermediate **M** was synthesized according to the literature[1].

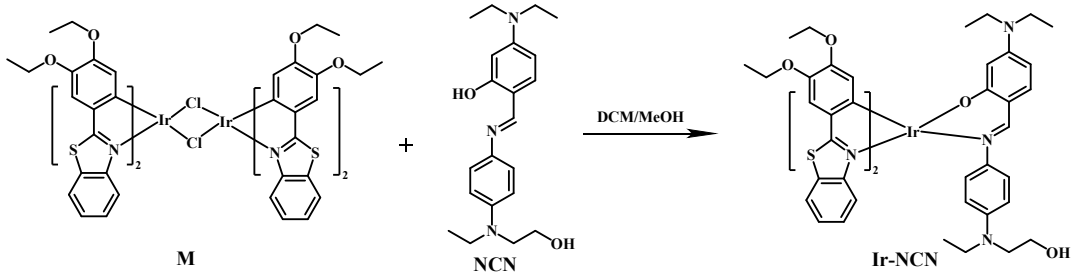

Figure. S4 The synthesis process of complex **Ir-NCN**.

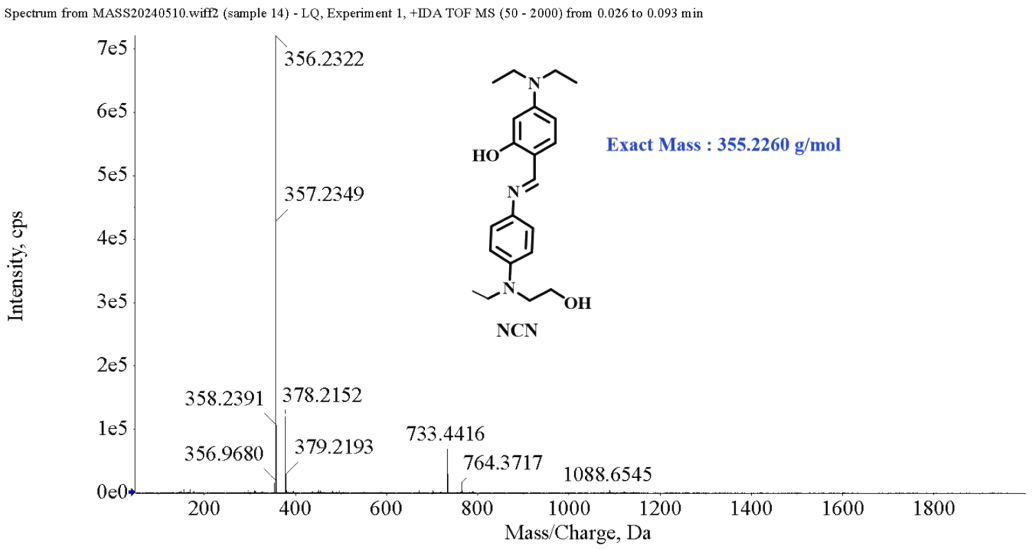

Figure. S5 MS spectrum of **NCN**.

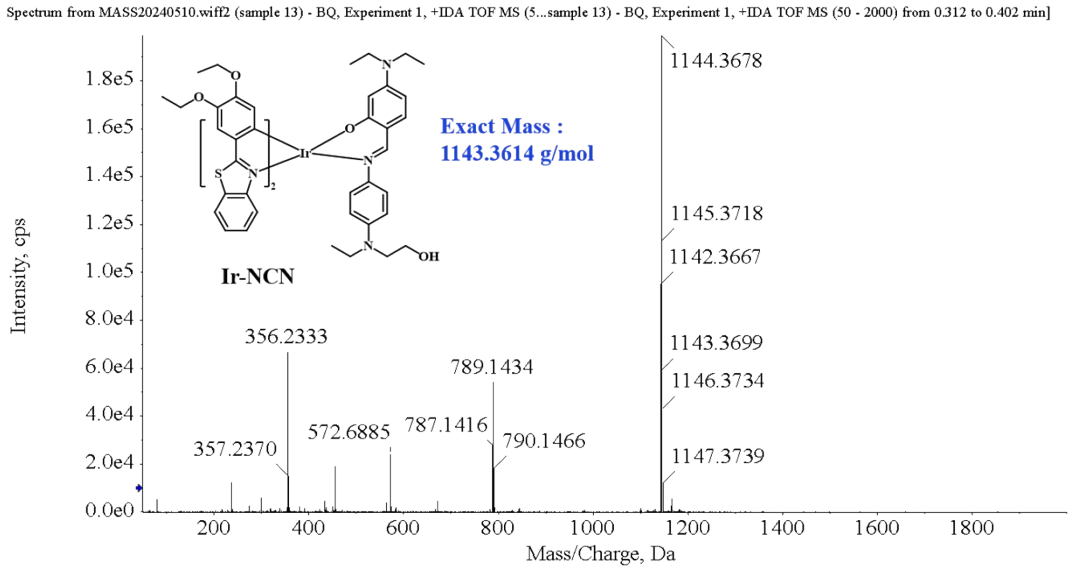

Figure. S6 MS spectrum of **Ir-NCN**.

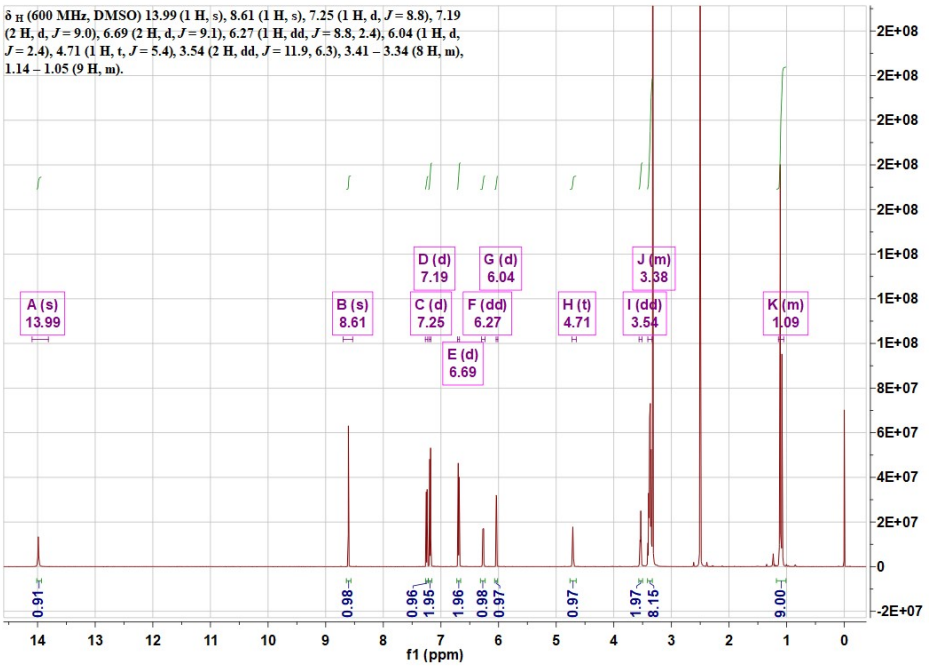

Figure. S7 [1]H-NMR spectrum of **NCN** in d_6-DMSO.

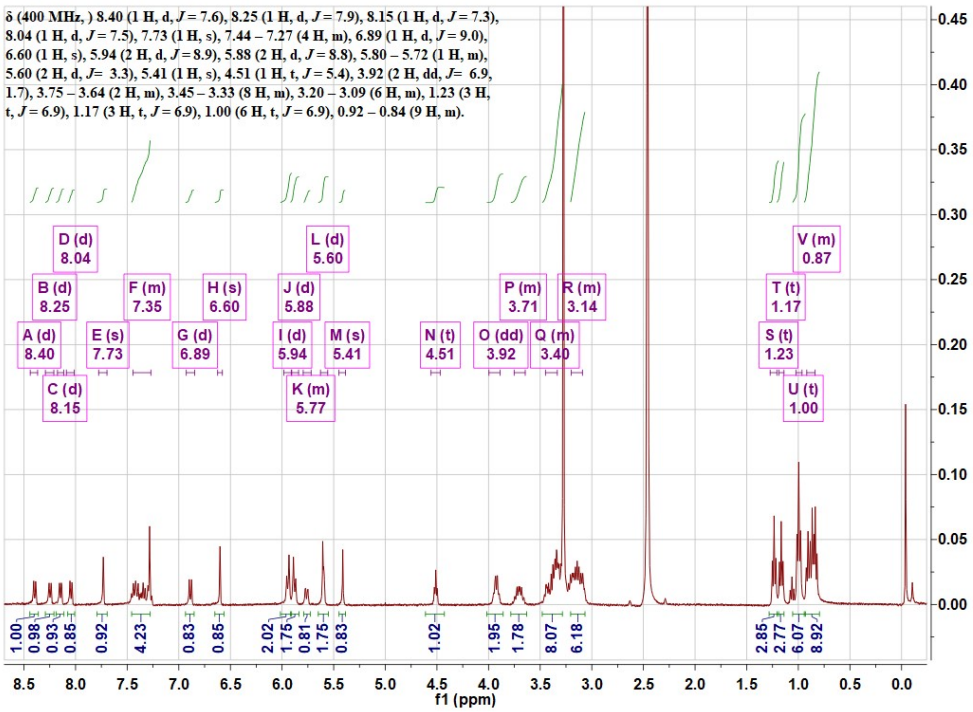

Figure. S8 [1]H-NMR spectrum of **Ir-NCN** in d_6-DMSO.

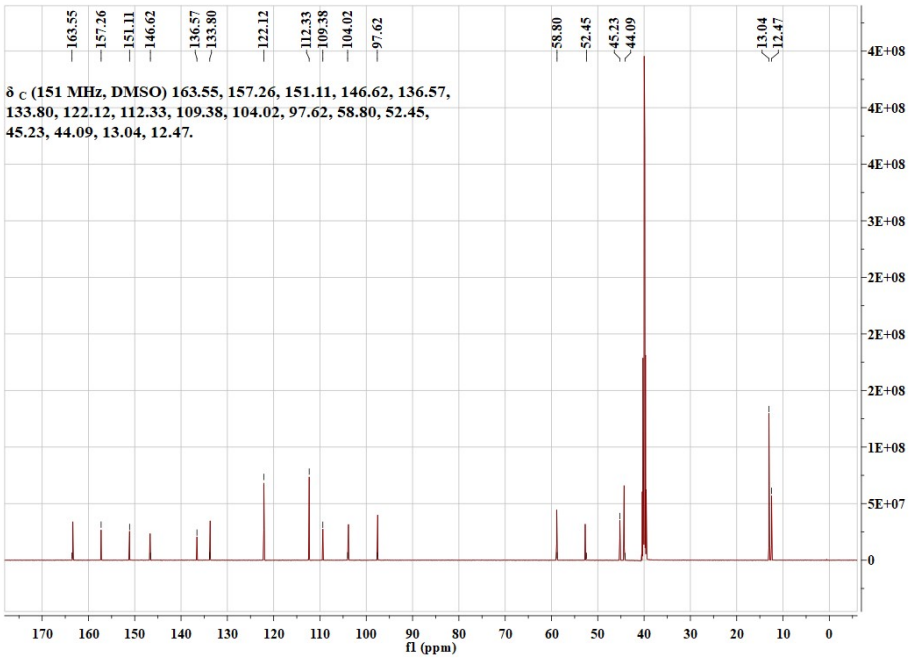

Figure. S9 ^{13}C-NMR spectrum of **NCN** in d_6-DMSO.

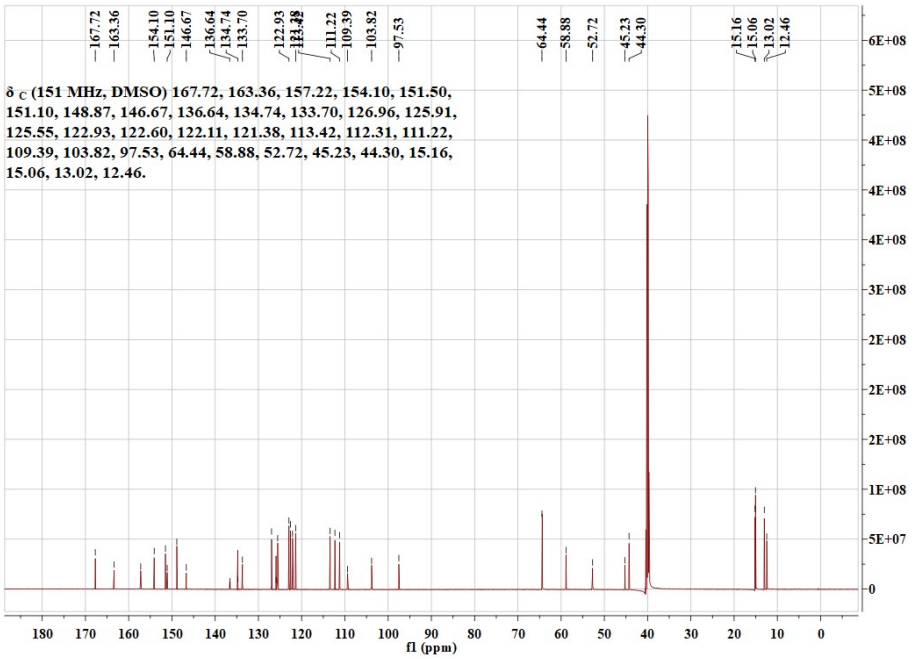

Figure. S10 ^{13}C-NMR spectrum of **Ir-NCN** in d_6-DMSO.

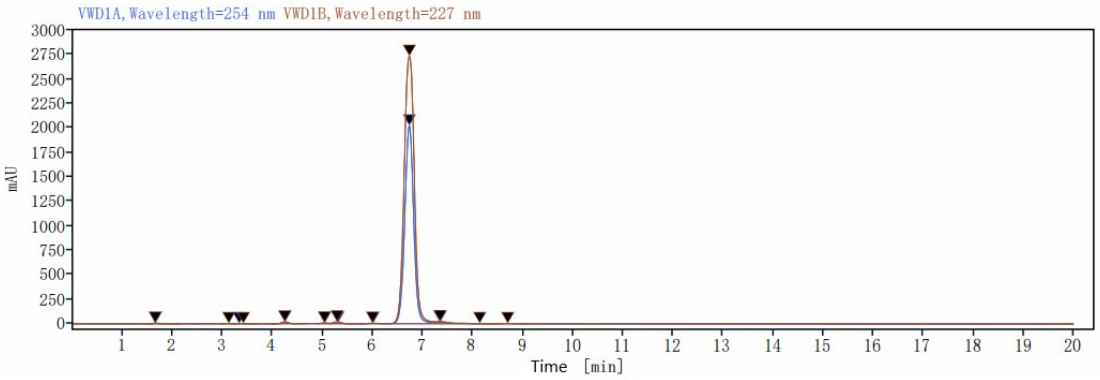

Figure. S11 HLPC spectrum of complex **Ir-NCN** monitored at 254 nm (acetonitrile (80%) as eluent, and retention time of complex **Ir-NCN** is 6.732 min).

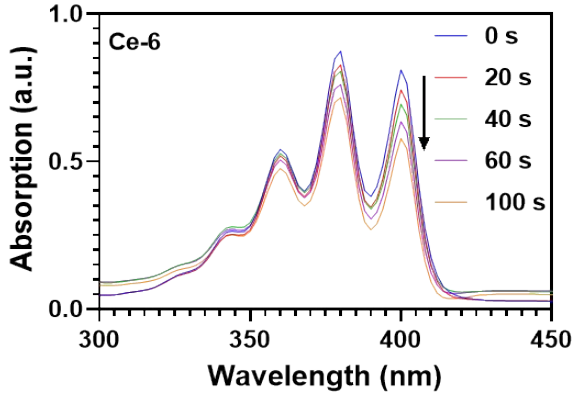

Figure. S12 Absorbance decay of ABDA (10 mM, PBS) in the presence of Ce-6 (10 μM) at different irradiation times.

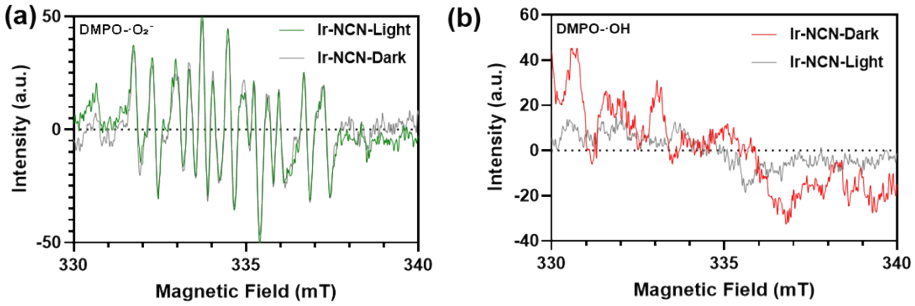

Figure. S13 ESR spectra of (a) DMPO-·O_2^- and (b) DMPO - ·OH generated by **Ir-NCN** (10 μM, DMSO) under LED laser irradiation (400-700 nm, 10 mW cm^{-2}, 1 min).

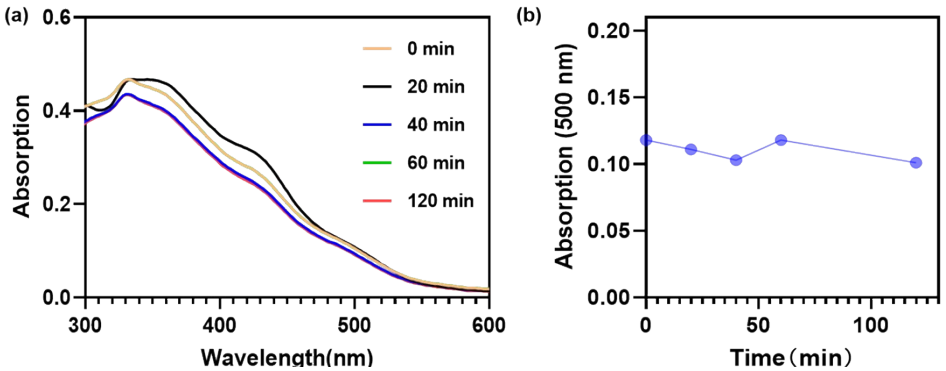

Figure. S14 (a) UV-*Vis* absorption spectra of the complex **Ir-NCN** in aqueous medium (with 1% DMSO) under LED light irradiation (400-700 nm, 10 mW·cm^{-2}) for different time intervals (0, 20, 40, 60, and 120 min). (b) The corresponding absorbance intensity at 500 nm as a function of irradiation time.

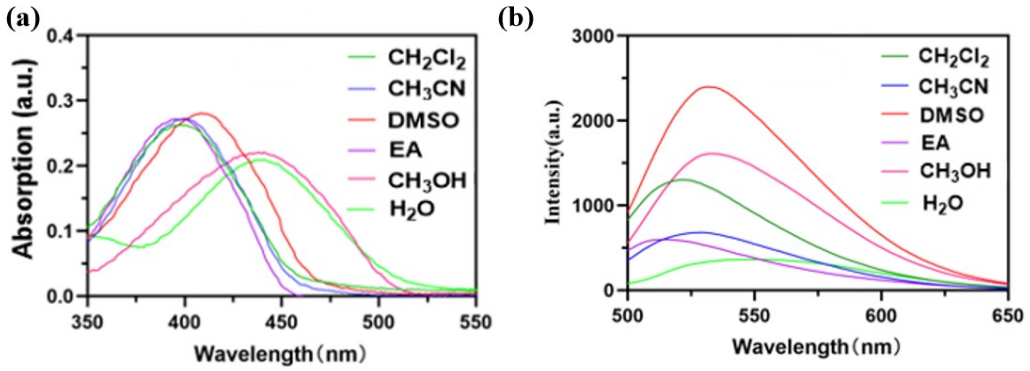

Figure. S15 The UV-*vis* absorption (a) and emission spectra (b) of the ligand **NCN** in solvents of different polarities.

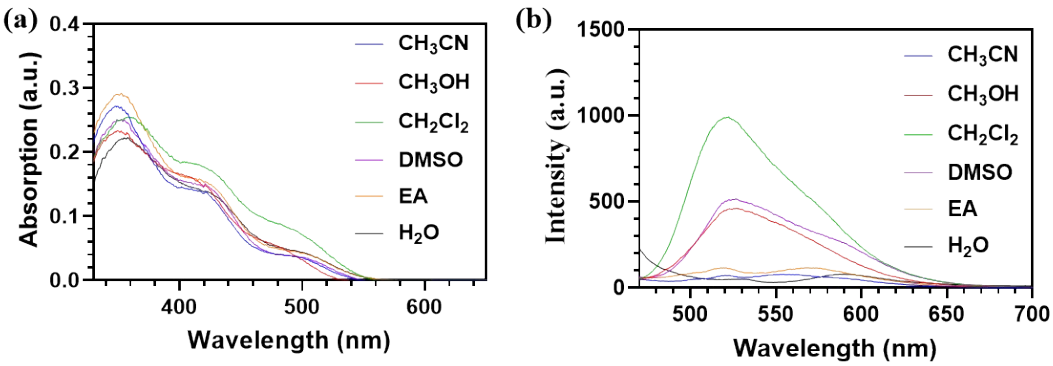

Figure. S16 The UV-*vis* absorption (a) and emission spectra (b) of the complex **Ir-NCN** in solvents of different polarities.

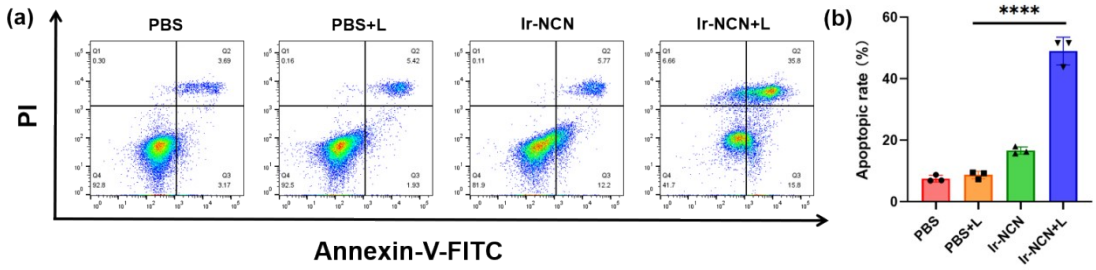

Figure. S17 (a) Cell apoptosis assay of 4T1 cells treated with **Ir-NCN** (10 μm) with or without light irradiation via Annexin V/PI staining. (b) Bar graph of quantitative statistics for each group. Results were presented as mean ± SD (n = 3, ****p < 0.0001).

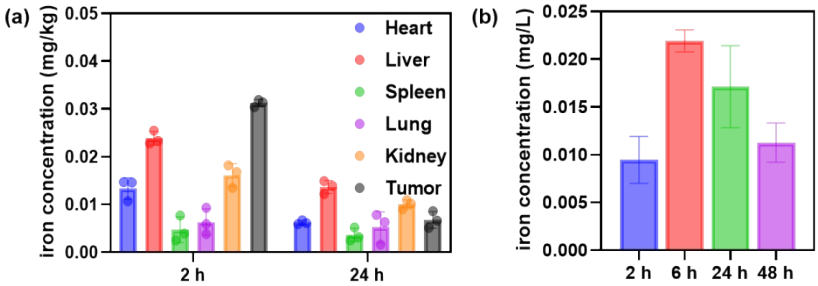

Figure. S18 (a) The biodistribution in major organs (heart, liver, spleen, kidney, lung) and tumors at 2 h and 24 h was determined using ICP-MS. (b) Concentration of iridium in the mice blood after intravenous injection of **Ir-NCN** (n=3).

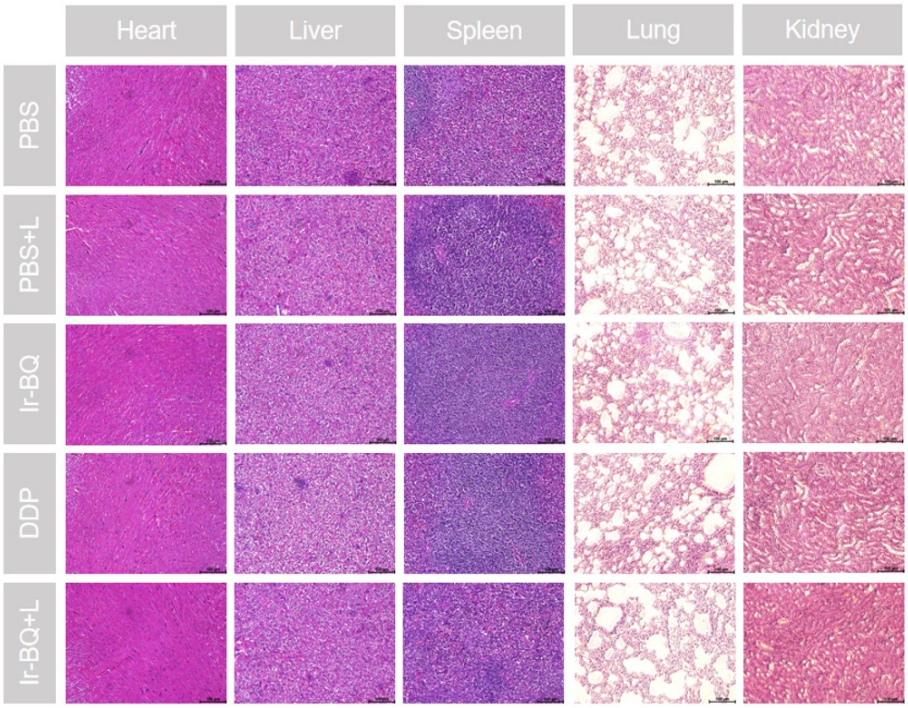

Figure. S19 H&E-stained images of major organ sections (heart, liver, spleen, lung, kidney) from 4T1 tumor-bearing mice (scale bar: 50 μm).

Table S1 The calculation results of $^1O_2$ generation capability

Comp.	NCN	Ir-NCN	Ce-6	RB
K	0.0004	0.00171	0.00138	0.0041
A	13.78	8.22	10.62	10.40
Φ	0.0055	0.39	0.25	0.75

Table S2 $^1O_2$ quantum yields of various photosensitizers

Complexes name	λ_{ex}(nm)	Φ($^1O_2$)	Reference
Ir1	413 nm	0.076	Sens. Actuators B Chem., 2025, 437, 137741.
Ir2	429 nm	0.275	
Ir3	450 nm	0.036 (RB as reference)	
1a-4a	360-550 nm	1a-4a: 0.13-0.80 1b: 0.51	JACS Au., 2025, 5, 6, 2825-2836.
1b-4b	360-550 nm	2b-4b: 0.82-0.98 ($Ru(bpy)_3]Cl_2$ as reference)	
$Ir(ppy)_3$	400 nm	0.50	Inorg. Chem.. 2025, 64, 14, 6898-6911.
Ir-COOH	400 nm	0.44	
Ir-PNA	400 nm	0.54 ($Ru(bpy)_3]Cl_2$ as reference)	
IrC2	379 nm	Not mentioned	J. Inorg. Biochem., 2025, 262, 112760.
IrC4	376 nm		
IrC6	380 nm		
IrC8	383 nm		
IrC12	386 nm		
Ir-S-S-Ir	492 nm	0.76	Inorg. Chem., 2024, 63, 50, 24030–24040.
Ir-C-C-Ir	488 nm	0.31	
Ir-C	489 nm	0.023 (MB as reference)	
Comlpex 1	392 nm	0.58	Dalton Trans., 2024,53, 17934-17947.
Comlpex 2	438 nm	0.76	
Comlpex 3	430 nm	0.64	
Comlpex 4	441 nm	0.60 ($Ru(bpy)_3]Cl_2$ as reference)	
IRDI	365 nm	0.49	ACS Appl. Bio Mater., 2023, 6, 12, 5776-5788.
IRMO	365 nm	0.28 ($Ru(bpy)_3]Cl_2$ as reference)	
Ir1@DEDTC	405 nm	0.281	Inorg. Chem., 2023, 62, 20080-20095.
Ir1@MORDTC	405 nm	0.239	
Ir1@MEDTC	365 nm	0.271	

Ir2@DEDTC	450 nm	0.864	
Ir2@MORDTC	450 nm	0.705 (MB as reference)	
Ir-Biotin	400nm	0.19 (MB as reference)	J. Mater. Chem. B., 2022,10, 5765-5773.
LDIr1	405 nm	0.79	Dyes Pigm., 2022, 203, 110387.
LDIr2	405 nm	0.84 ($Ru(bpy)_3]Cl_2$ as reference)	
BODIPY-Ir	500 nm	0.35 (RB as reference)	Dalton. Trans., 2021, 50, 14332-14341.
Ir-OH	500 nm	0.31	Inorg. Chem. Front., 2021, 8, 5045-5053.
Ir-$B(OH)_2$	405 nm	0.32 (RB as reference)	
1a-FCPF	467 nm	0.51	
2a-FCPF	473 nm	0.45	
3a-FCPF	419 nm	0.55	Inorg. Chem., 2020, 59, 14796.
4a-FCPF	419 nm	0.54	
5a-FCPF	440 nm	0.69	
6a-FCPF	438 nm	0.63 (MB as reference)	
NIR-Ir-XE	510 nm	0.75 ($Ru(bpy)_3]Cl_2$ as reference)	Biomater. Sci., 2021,9, 4843-4853.
This work Ir-NCN	450nm	0.39 (RB as reference)	

References:

[1] B. Ni, H. Z. Cao, C. K. Zhang, S. L. Li, Q. Zhang, X. H. Tian, D. D. Li, J. Y. Wu and Y. P. Tian. Activated type I and type II process for two-photon promoted ROS generation: the coordinated Zn matters. *Inorg. Chem*., 2020, **59**, 13671-13678.

[2] F. Li, C. L. Li, W. J. Huang, W. Y. Li, Y. Q. Zhang, Z. B. Li, Y. Liu, J. B. Tong, D. Wang and Z. H. Feng. Rational design of iridium complex with double-locked mitochondria-targeting for dynamic viscosity monitoring and precision two-photon tumor imaging. *Sens. Actuators B Chem*., 2025, 442, 138145.